

October 1993

UT-652

Predictions on Two-dimensional Turbulence by Conformal Field Theory

H. Câteau, Y. Matsuo and M. Umeki

Department of Physics, University of Tokyo,
7-3-1 Hongo, Bunkyo-ku, Tokyo 113, Japan

(Received,)

Abstract

A generalized theory of two-dimensional isotropic turbulence is developed based on conformal symmetry. A number of minimal models of conformal turbulence are solved under an extended constraint including both the enstrophy cascade by Kraichnan and the discontinuity of vorticity by Saffman. There are an infinite number of solutions which fall into two different categories. An explicit relation is derived in one of the categories between the central charge of Virasoro algebra, the lowest anomalous dimension and the power of the energy spectrum. Some statistical properties such as energy spectrum, skewness, flatness and Casimir invariants are predicted and compared with numerical simulation by the pseudospectral method.

KEYWORDS: conformal field theory, two-dimensional turbulence

1 Introduction

The problem of the energy spectrum has still been controversial in two-dimensional turbulence. In three dimensions, dimensional analysis by Kolmogorov [19] shows that the energy spectrum in the inertial subrange should be scaled as $E(k) = C\epsilon^{2/3}k^{-5/3}$, where ϵ is the energy dissipation rate. Kraichnan [17], Leith [20] and Batchelor [1] applied Kolmogorov theory to the two-dimensional turbulence and obtained that a power of the energy spectrum should be -3 according to existence of the enstrophy cascade in the inviscid limit. On the other hand, Saffman [28] derived the power -4 of the energy spectrum by assuming the jump of constant- vorticity layers. A possible explanation of these difference is proposed by Gilbert [12] in which spiral structures of vortical region play an important role and may fill the gap between these two spectra.

In many of numerical simulations [16][3][29] of decaying two-dimensional turbulence with the initial gaussian spectrum, the power increases from -4 to -3 , contours of vorticity are stretched and an active enstrophy cascade is observed up to $t \approx 10$. Then coherent vortices emerge with spiral tails and the power of the energy spectrum decreases [23]. Moreover, a very long-time simulation [25] shows that in the final stage the flow seems to settle down to the universal "sinh" state with the maximum entropy, which is predicted by a statistical argument of the assembly of point vortices [24]. Analytical closure theories, such as direct interaction approximation (DIA) and test field model have been also applied to evaluate quantitatively the energy spectrum with its constant and the enstrophy transfer [18] [14] in a reasonable comparison with numerical results. Kraichnan [18] argues that the logarithmic correction can escape from the divergence of the enstrophy integral.

Recently, Polyakov [26] [27] has proposed that one may use the conformal field theory (CFT) to analyze two dimensional turbulence. Since there appears power law in the correlation functions of velocity fields, for example, the existence of the conformal invariance seems quite natural. The merit to use CFT is that there are well-classified models (minimal models) where there appears only finite number of independent operators. Usually, when we try to calculate n point functions, we need the knowledge of $n + 1$ point functions because of the nonlinearity of the Navier-Stokes equation. Since we can not usually cope with infinite number of degree of freedom, we need to restrict them to the physically relevant ones from outside, for example, quasi-normal and DIA theories. If the turbulence is described by CFT minimal models, such restriction comes from mathematical consistency and there are no arbitrariness. In the original paper, Polyakov proposed a minimal model (21,2) as the candidate which may describe turbulence. This model predicts quite a reasonable value for the exponent. However, it was indicated later by several groups [22][21][8][11] that Polyakov's condition on the CFT is not satisfied by unique model, but in fact there are infinite number of candidates. Also, as Polyakov himself discovered [27], there may be some ambiguities in the conditions for CFT if one considers the non-vanishing of one point functions in the system with boundaries. Even if one takes the modified conditions, the situation does not change and there are again a lot of CFT candidates.[6] In any case, if one can not find other appropriate conditions, one may not tell which model is more preferable. One can not even say whether there are several universality classes.

Due to appearance of infinite solutions, we can not predict uniquely the exponent of energy spectrum. In such situation, it is difficult to convince ourselves whether prediction from CFT is useful as long as we consider only one observable. One way to proceed in this situation is to consider the global (or geometrical) aspect of the conformal turbulence.[5] In this paper, we would like consider another direction. In CFT models, there appear a lot of primary fields beside

the original velocity field. It is quite important consider the physical meaning of these fields. Some of them can be obtained in the short distance expansion of the velocity field. Thus we can relate it to the the dependence of three or four point functions on the Reynolds number which is known as the “skewness” or “flatness”. If the assumption of the local equilibrium is correct, they should be some universal constants. However, in CFT, we get nontrivial dependence on Reynolds number due to the anomalous dimension. In three-dimensional turbulence, there is a tendency that both skewness and flatness of velocity derivatives increases as Reynolds number becomes large [30]. In many of CFT solutions, however, the behavior is the opposite to these three-dimensional observations.

Interestingly, as we prove in this paper, these exponents are not independent with each other but can be uniquely determined from the exponent of energy spectrum. This property is tightly related to the finiteness of minimal models. Intuitively, in order to calculate the higher correlation functions, the most dominant contribution comes from the lowest dimension operator in the OPE. However, in the minimal models, there are always lower bound in the dimensions of primary fields. We surveyed more than 1600 candidates of CFT solutions. In 99% of them, the lowest dimension is attained in the first OPE between $\psi \times \psi$. The other 1% behaves quite differently but we show that they can be determined exactly.

As another peculiar character, two-dimensional inviscid flows possess infinite number of conserved quantities $\langle \omega^n \rangle$ which are topological invariants of area-preserving diffeomorphism, called Casimir. It is commonly believed that these conservation laws may affect the character of the two-dimensional turbulence, i.e. ergodicity, energy spectrum and so on, although the effects are not fully understood. A finite-mode system of two-dimensional Euler flow preserving such conservation laws is derived by Zeitlin[32]. However, the effect of this conservation laws on the behavior of turbulent states is still unresolved. Using CFT theories, Falkovich and Hanany[9] showed that the dependence of the dissipation rate of $\langle \omega^n \rangle$ on the viscosity ν can be predicted. We extend their results and compare the prediction with the numerical results.

This paper is organized as follows. In section 2 we review the classical theories of two-dimensional turbulence. It is shown that the extended theory, which contains both the Kraichnan-Leith-Batchelor’s and Saffman’s theories, is useful in order to understand the conformal turbulence. In section 3 Polyakov’s conformal turbulence is reviewed with a brief sketch of conformal field theory. The original CFT models are generalized so that the imposed constraint includes not only the Kraichnan’s constant transfer of enstrophy but also the non-cascade theory by Saffman. In section 4 solutions of this generalized CFT models of two-dimensional turbulence are shown. Distributions of the energy spectra are revealed, A relation between the central charge in CFT and the power of the energy spectrum is described. In section 5 higher order statistics including

skewness and flatness factors are derived. Scaling of Casimir invariant $\langle \omega^n \rangle$ and its decay rate are discussed in section 6. These predictions are compared with the numerical simulations in section 7. Conclusions and discussions are summarized in section 8. Throughout this paper, attention is paid on removal of the gap between the field theory and fluid communities.

2 Theories of two-dimensional turbulence

We shall review standard theories of two-dimensional turbulence in order to understand the conformal theory of it. In what follows we mainly keep in mind the decaying turbulence, i.e. the system with no external forcing. The equations governing the two-dimensional incompressible viscous flow are

$$\frac{\partial \mathbf{v}}{\partial t} + (\mathbf{v} \cdot \nabla) \mathbf{v} = -\nabla p + \nu \Delta \mathbf{v}, \quad (1)$$

$$\nabla \cdot \mathbf{v} = 0. \quad (2)$$

The vorticity equation is given by

$$\frac{\partial \omega}{\partial t} + J(\psi, \omega) = \nu \Delta \omega, \quad (3)$$

where ψ is the streamfunction, $\omega = -\Delta \psi$ is the vorticity, and the Jacobian J is defined by

$$J(\psi, \omega) = \frac{\partial \psi}{\partial y} \frac{\partial \omega}{\partial x} - \frac{\partial \psi}{\partial x} \frac{\partial \omega}{\partial y}. \quad (4)$$

From (1) and (3), the evolution of total energy $E = \frac{1}{2} \langle |\mathbf{v}|^2 \rangle$ and square-vorticity, called enstrophy $\Omega = \frac{1}{2} \langle \omega^2 \rangle$, is given by

$$\frac{dE}{dt} = -2\nu\Omega \equiv -\varepsilon, \quad (5)$$

$$\frac{d\Omega}{dt} = -2\nu P \equiv -\eta, \quad (6)$$

Because the enstrophy decreases monotonically, the energy dissipation rate ε vanishes in the inviscid limit $\nu \rightarrow 0$. Thus the stationary energy cascade is irrelevant in decaying two-dimensional turbulence, although in the forced system, the energy is transferred to the low wavenumber side, called the inverse cascade.

In Kraichnan-Leith-Batchelor theory, the turbulence is characterized by the cascade of enstrophy. The dimensional analysis shows the energy spectrum is expressed as

$$E(k) = C\eta^{2/3}k^{-3}, \quad (7)$$

in the inertial subrange $L^{-1} \ll k \ll \delta^{-1}$ where η is the enstrophy dissipation rate, C is a universal constant, L denotes the large scale length which may be considered as the size of the largest eddy of coherent structures or the boundary condition, and δ implies the dissipation scale given by

$$\delta = \nu^{1/2} \eta^{-1/6}. \quad (8)$$

The total energy estimated by the integral in the inertial range leads to

$$E = \int_{L^{-1}}^{\delta^{-1}} E(k) dk = \frac{1}{2} C \eta^{2/3} L^2. \quad (9)$$

On the other hand L may be evaluated by E and Ω as

$$L = \left(\frac{E}{\Omega} \right)^{1/2}. \quad (10)$$

From (9) and (10) we may obtain the Reynolds number as

$$Re \equiv \frac{E}{\nu \sqrt{\Omega}} \approx \left(\frac{L}{\delta} \right)^2. \quad (11)$$

In this theory η and ν are considered as independent and it is allowed that η remains finite in the inviscid limit.

Saffman considered that, in the context of decaying two-dimensional turbulence, the discontinuity of the vorticity is the asymptotic feature by extending the argument of one-dimensional turbulence, i.e. Burgers equation. The energy spectrum may be given by

$$E(k) = \frac{\Omega}{2L} k^{-4}, \quad L^{-1} \ll k \ll \delta^{-1}, \quad (12)$$

and the dissipation length is given by

$$\delta = \frac{(\nu L)^{1/3}}{\Omega^{1/6}}. \quad (13)$$

The enstrophy dissipation rate is estimated as

$$\eta = \frac{\nu^{2/3} \Omega^{7/6}}{L^{4/3}}. \quad (14)$$

Using $L^2 \Omega = E$ and E remains constant in the inviscid limit, (14) is rewritten as

$$\eta = \frac{\nu^{2/3} \Omega^{11/6}}{E^{2/3}}. \quad (15)$$

Thus η depends on ν as $\nu^{2/3}$. By Saffman's picture there is no enstrophy cascade in the inviscid limit. Reynolds number is given by

$$Re = \left(\frac{L}{\delta} \right)^3. \quad (16)$$

Comparing the energy spectra and the dissipation lengths of the two theories, it seems quite useful to develop a following extended theory. That is, the energy spectrum in the inertial range is given by

$$E(k) = \frac{\Omega}{2} L^{\alpha+3} k^\alpha, \quad L^{-1} \ll k \ll \delta^{-1}, \quad (17)$$

and the dissipation scale is expressed as

$$\delta = L \left(\frac{\nu}{\sqrt{\Omega} L^2} \right)^\beta, \quad (18)$$

where parameters α and β are introduced in order to bridge over the two standard theories. This generalization is also important when we consider CFT turbulence described in the following section.

From (18), the Reynolds number is estimated as

$$Re = \left(\frac{L}{\delta} \right)^{1/\beta}. \quad (19)$$

The enstrophy dissipation rate η is estimated as

$$\eta = 2\nu \int_{L^{-1}}^{\delta^{-1}} k^4 E(k) dk \approx \frac{\nu \Omega L^{\alpha+3}}{\delta^{\alpha+5}}. \quad (20)$$

Substituting (18) into (20) the dependence of η on Ω, ν, L is expressed as

$$\eta \approx \Omega^{1+\gamma/2} \nu^{1-\gamma} L^{-2+2\gamma}, \quad (21)$$

where $\gamma = \beta(\alpha + 5)$. Using (10) η is expressed by Ω, ν , and E as

$$\eta \approx \frac{\Omega^2 \nu}{E} \left(\frac{E}{\nu \sqrt{\Omega}} \right)^\gamma. \quad (22)$$

Moreover, the restrictions

$$(\alpha, \beta) = (-3, \frac{1}{2}), \quad (\gamma = 1), \quad (\alpha, \beta) = (-4, \frac{1}{3}), \quad (\gamma = \frac{1}{3}), \quad (23)$$

may be imposed if this extension should meet both the enstrophy cascade theory and Saffman's spectrum.

A more physical argument, which reconcile the two theories similarly to our idea, is made by Gilbert [12], who showed that the energy spectra with powers between -3 and -4 can be derived by considering that the isolated strong vortex cores wind up the discontinuous lines of the vorticity. This spiral model gives the energy spectrum in the inertial subrange as

$$E(k) \approx (\Gamma t)^{2/(s+1)} k^{-4+(s-1)/(s+1)}, \quad (24)$$

where Γ denotes the strength of the vortex and the parameter s specifies the distribution of the vorticity in the core. The value of s is allowed as $1 < s < \infty$, $s = 1$ implies the Saffman's power

-4 , $s = \infty$ gives the KLB values -3 and the index of the realistic vortex is approximately 2 (the value of the point vortex), which gives the power $-11/3$.

In the case of decaying turbulence, the temporal behavior of Ω can be obtained by integrating (22) assuming that E is nearly constant:

$$\Omega(t) = \left[\Omega(0)^{-1+\gamma/2} + \left(1 - \frac{\gamma}{2}\right) \left(\frac{\nu}{E}\right)^{1-\gamma} t \right]^{\frac{2}{\gamma-2}}. \quad (25)$$

Thus the enstrophy decays at large t as

$$\Omega \approx \left(\frac{\nu}{E}\right)^{\frac{2(1-\gamma)}{\gamma-2}} t^{\frac{2}{\gamma-2}}, \quad (26)$$

and the enstrophy dissipation rate becomes

$$\eta \approx \left(\frac{\nu}{E}\right)^{\frac{\gamma(1-\gamma)}{\gamma-2}} t^{\frac{4-\gamma}{\gamma-2}}. \quad (27)$$

These are consistent with $\Omega \sim t^{-2}, \eta \sim t^{-3}$ of Batchelor if $\gamma = 1$ and $\Omega \sim t^{-6/5}, \eta \sim t^{-11/5}$ of Saffman if $\gamma = 1/3$.

We are also interested in the behavior of the infinite number of inviscid invariants, i.e., arbitrary powers of vorticity, in the limit $\nu \rightarrow 0$. The decay rate of $\Omega_n \equiv \frac{1}{2} \langle \omega^n \rangle$ is given by

$$\eta_n \equiv -\frac{d\Omega_n}{dt} = \frac{n(n-1)\nu}{2} \langle \omega^{n-2} (\nabla \omega)^2 \rangle. \quad (28)$$

It is difficult to get the dependence of η_n on Ω and η , but if we assume a random phase distribution of the Fourier coefficients of ω , we get the dependence as

$$\eta_n = 2^{\frac{n}{2}-1} n(n-1)(n-3)!! \nu \Omega^{\frac{n}{2}-1} P \propto \Omega^{\frac{n}{2}-1} \eta, \quad (29)$$

for an even n and $\eta_n = \Omega_n = 0$ for an odd n . From (26), (27) and (29), η_n decays as

$$\eta_n \propto \left(\frac{\nu}{E}\right)^{\frac{(1-\gamma)[n-2+\gamma]}{\gamma-2}} t^{\frac{n+2-\gamma}{\gamma-2}}. \quad (30)$$

The pair $(\alpha, \beta) = (-3, 1/2)$ gives

$$\eta_n \sim t^{-n-1},$$

and $(\alpha, \beta) = (-4, 1/3)$ leads to

$$\eta_n \sim (E/\nu)^{(6n-10)/15} t^{-1-3n/5}.$$

Thus the dissipation rate of Ω_{2n} is independent of viscosity by the enstrophy cascade theory and increases as ν tends to zero by Saffman's picture in the random phase approximation.

3 Conformal turbulence

3.1 Short summary of CFT

In order to make smooth communication between fluid dynamics and elementary particle community, we would like give a short sketch of some basics of CFT. The material is quite standard. See the original paper to understand the detail[2]. Also there are many nice review articles, for example, see [15].

In quantum field theory, symmetry generally plays an important role. On the one hand symmetry implies existence of conservation law and resulting in effective reduction of the degrees of freedom. On the other hand, symmetry is a useful tool to select out nicely behaving class of field theories among vast amount of all the possible field theories.

The most successful example of such is the class of two dimensional conformal field theories (CFT). The field theory in the class is defined in two dimension, and has the conformal invariance as its symmetry. This means, if we use a complex variable $z = x_1 + ix_2$, dynamics of theory is invariant under an complex analytic transformation $z' = f(z)$. Polyakov et al. [2] performed a systematic study of CFT and showed that the conformal symmetry is really powerful to classify possible CFTs and solve them.

Physically, CFT concerns the critical point of the second order phase transition of statistical systems. On the critical point, we are faced with the situation that the correlation length of the operators in the system grows up to infinity. In this limit, the system gains the conformal invariance. Then the two dimensional system is described by CFTs.

Especially in two dimensions, it is known that the conformal symmetry becomes infinite dimensional and generated by the operators L_n and \bar{L}_n ($n = 0, \pm 1, \pm 2, \dots$). They form a Lie algebra:

$$[L_n, L_m] = (n - m)L_{n+m} + \frac{c}{12}(n^3 - n)\delta_{n+m,0}, \quad (31)$$

which is called Virasoro algebra. The last term in the RHS comes from quantum anomaly.

Important fact is that we have a detailed understanding of its representations theory, and he knowledge is really helpful in classifying all the possible CFTs. Representation theory is quite different whether $c \geq 1$ or $c < 1$. In the former case, the classification of the possible theories is not completely done with Virasoro algebra alone, we need further informations such as the extended symmetry to classify and solve the system. Conversely, in the latter case, the Virasoro algebra is strong enough to completely classify all the possible theories and to solve the system completely. In fact, it was shown that the central charge is restricted to take only the discrete values,

$$c = 1 - \frac{6(p - q)^2}{pq}, \quad (32)$$

with (p, q) mutually coprime integers. These models are so-called minimal models.

In CFT, we have two kinds of fields called primary fields and secondary fields. The former is covariant under the conformal transform,

$$\phi_{\Delta\bar{\Delta}}(z, \bar{z}) \rightarrow \left(\frac{\partial w}{\partial z}\right)^\Delta \left(\frac{\partial \bar{w}}{\partial \bar{z}}\right)^{\bar{\Delta}} \phi_{\Delta\bar{\Delta}}(w, \bar{w}), \quad (33)$$

while the latter is not. For each primary field, there are infinite number of secondary fields. Those can be obtained from the primary field through the action of the Virasoro generators. Derivative of the primary field is a typical secondary field.

One of the most important properties of the minimal model is that the number of primary fields is finite. For the minimal model characterized by p, q , the conformal dimensions Δ ($\bar{\Delta}$) of primary fields are restricted to take the following discrete values,

$$\Delta_{rs} \equiv \frac{(ps - qr)^2 - (p - q)^2}{4pq} \quad 1 \leq r \leq p - 1, \quad 1 \leq s \leq q - 1, \quad ps > qr. \quad (34)$$

The final restriction $ps > qr$ comes from the fact that we can identify primary field with label (r, s) and $(p - r, q - s)$. This set of primary fields is called the Kac table.

It may be intuitive to compare the representation of the Virasoro algebra with that of $su(2)$ algebra.¹ The primary field described above corresponds to the highest weight state in the $su(2)$ representation. The states generated from highest weight state by the action of lowering operator should be compared to the secondary field. Finally, corresponding to the composition rule of the angular momenta, two primary fields are composed to give several other primary fields. Namely the primary fields form an algebra by the composition operation. The composition rule is called fusion algebra or operator product expansion, OPE.

The rule can be deduced from the representation theory just like the computation of the Clebsh-Gordan coefficients of $su(2)$ representation. For the Virasoro algebra, the OPE is explicitly given by,

$$\phi_{r's'} \times \phi_{r''s''} \sim \sum_{r=|r'-r''|+1}^{\min(r'+r''-1, 2p-r'-r''-1)} \sum_{s=|s'-s''|+1}^{\min(s'+s''-1, 2q-s'-s''-1)} [\phi_{rs}], \quad (35)$$

where $\phi_{r,s}$ denotes the primary field whose conformal dimension is Δ_{rs} . The symbol $[\]$ denotes the conformal family (the primary field and its associated secondary fields). If we regard (35) as the short distance expansion, the contribution from the secondary fields are higher order in power of $z\bar{z}$ compared to those coming from the primary field, so they are irrelevant.

Finally, let us see some examples of CFT. The minimal models are not necessarily unitary. In other words, negative norm state appears in some situations. Only if $p = q + 1 = m + 1$ with

¹ There are no object in $su(2)$ algebra which correspond to the central charge of the Virasoro algebra. This term originates from the infinite dimensionality of the algebra.

$m = 2, 3, 4, \dots$, the theory is unitary. Many of the critical points of the known 2-dim statistical systems are described by the models in this series. For example, the Ising model ($c = 1/2$, i.e. $m = 3$) the tri-critical Ising model ($c = 7/10$, i.e. $m = 4$), the three state Potts model ($c = 4/5$, i.e. $m = 5$), and so on. For these models, one can find the physical interpretation for the primary fields. For example, for Ising model, we have three independent primary operators,

$$\Delta_{11} = 0 \quad \Delta_{21} = 1/16 \quad \Delta_{31} = 1/2.$$

These operators may be identified with, identity operator, energy density and the spin field respectively.

On the other hand, the nonunitary models are by no means physical, but contains some very interesting models, such as Yang-Lee edge singularity ($c = -22/5$, i.e. $(p, q) = (5, 2)$). They are characterized by the appearance of the negative dimension operators. For the Yang-Lee edge singularity case, we have $\Delta_{2,1} = -1/5$. In the unitary case, the lowest dimension operator in the system is always the vacuum, which is represented by the primary field with $\Delta_{1,1} = 0$. For the non-unitary case, this 'vacuum' is no longer the lowest dimension operator but rather we have a primary field with dimension,

$$\Delta_0 = \frac{1 - (p - q)^2}{4pq}. \quad (36)$$

This operator may be regarded as the 'true vacuum' of the system.

Let us take a nonunitary model $(p, q) = (21, 2)$ as an example. Field content consists of ten fields: $\phi_{1,1}, \phi_{2,1}, \dots, \phi_{10,1}$. Since the second index s is always unity in this case, we will omit it hereafter. OPE is, for example

$$\phi_4 \times \phi_4 \sim [\phi_7] + [\phi_5] + [\phi_3] + [\phi_1]. \quad (37)$$

For the two point function, this fusion rule implies that

$$\begin{aligned} \langle \phi_4(z) \phi_4(0) \rangle &= (z\bar{z})^{2\Delta_7 - 4\Delta_4} \langle \phi_7(0) \rangle + \dots + (z\bar{z})^{2\Delta_1 - 4\Delta_4} \langle \phi_1(0) \rangle \\ &\quad + \text{higher order terms w.r.t. } z\bar{z}. \end{aligned} \quad (38)$$

Note that z, \bar{z} dependence of each term in RHS is determined by the accordance of the length dimension in both sides.

3.2 Conformal Turbulence

3.2.1 Polyakov's original definition

In CFT approach to two dimensional turbulence, the fluid circulation function ψ is supposed to be described by a primary field of a minimal model of CFT. ψ is related to the velocity field through $v_\alpha = \epsilon_{\alpha\beta} \partial_\beta \psi$. Polyakov's conditions for CFT to describe turbulence are following,

1. Hopf equation should be satisfied,

$$\langle \epsilon_{\alpha\beta} \partial_\alpha \psi \partial^2 \partial_\beta \psi \dots \rangle = 0. \quad (39)$$

2. Constant flow of enstrophy in the momentum.

Assuming operator product expansion (OPE),

$$[\psi] [\psi] \sim [\phi] + \dots, \quad (40)$$

where ϕ is the smallest dimension primary field in OPE, the nonlinear term in the Navier-Stokes equation (39) is equivalent to

$$|a|^{2\Delta_\phi - 4\Delta_\psi} (L_{-2} \bar{L}_{-1}^2 - \bar{L}_{-2} L_{-1}^2) \phi, \quad (41)$$

where a is a viscous cutoff length. Vanishing of this quantity then produces either

$$2\Delta_\phi - 4\Delta_\psi > 0, \quad (42)$$

or $L_{-2}\phi \sim L_{-1}^2\phi$. The second equation (which is equivalent to that ϕ is (2,1) type primary field) is not compatible with the conditions on enstrophy and Polyakov has picked up the first condition.

The constant enstrophy flow constraint is more subtle. The time derivative of the enstrophy gives

$$\frac{\partial \Omega}{\partial t} = \langle \omega \phi^{(2)} \rangle, \quad (43)$$

with $\omega = \partial^2 \psi$ and $\phi^{(2)} = (L_{-2} \bar{L}_{-1}^2 - \bar{L}_{-2} L_{-1}^2) \phi$. Rewriting the right hand side of (43) as the integral in the momentum space, the constant enstrophy condition is equivalent to

$$\langle \omega(x) \phi^{(2)}(0) \rangle \sim x^0. \quad (44)$$

Naive dimensional counting shows that it is equivalent to $\Delta_\psi + \Delta_\phi + 3 = 0$. However, we have to be careful to the contribution of the one point function, which is non-vanishing in the general topology of two dimensional space. The dependence of one point function on the characteristic length of the system is

$$\langle \psi \rangle = L^{-2\Delta_\psi}, \quad (45)$$

for any primary field ψ . For unitary theory where dimension of any primary field is positive, one point function is not relevant in the large L limit. However, since we are discussing on the system where dissipation takes place, we are dealing with non-unitary theory where negative dimensional operator appears. In this situation, the lowest dimension operator becomes most relevant one. If

we denote χ as the lowest dimension primary field in OPE $[\psi][\phi]$, then the correct condition for the constant enstrophy flow is

$$\Delta_\psi + \Delta_\phi - \Delta_\chi + 3 = 0. \quad (46)$$

The solutions of CFT that satisfy (42) and (46) was discussed by Chung et. al.[6] and they found several hundreds candidates.

Once we know that there are solutions, the next step is how to extract physical exponents out of them. The most important one is discussed by Polyakov, i.e. the exponent of energy spectrum, which may be described by,

$$E = \int dk E(k) = \frac{1}{2} \sum_{\mu=1}^2 \langle v^\mu v^\mu \rangle. \quad (47)$$

From contribution of the one-point function (45), one finds that

$$E(k) \sim k^\alpha, \quad \text{with } \alpha = 4\Delta_\psi - 2\Delta_\phi + 1. \quad (48)$$

If the one-point correlation integral vanishes, the energy spectrum becomes

$$E(k) \sim k^\alpha, \quad \text{with } \alpha = 4\Delta_\psi + 1. \quad (49)$$

These expressions are Fourier transform of two-point functions,

$$\langle \psi(z)\psi(0) \rangle \sim |z|^{-4\Delta_\psi}, \quad (50)$$

for correlation function on sphere [2] and

$$\langle \psi(z)\psi(0) \rangle \sim L^{-2\Delta_\phi} |z|^{-4\Delta_\psi + 2\Delta_\phi}, \quad (51)$$

for correlation function on general topology Riemann surface including torus. This kind of correlation functions was discussed previously by J. Cardy [4] which is the refinement of the discussion given by Fisher [7]. The correlation function of unitary model (in particular, Ising model) on the torus was obtained explicitly by Di Francesco et. al.[10]. In the turbulence context, some of the physical implication was discussed by Polyakov[27] and Chung et.al. [5] and [6]. The most important observation is that we can not neglect the contribution of the one point function. This is because the dimension of ϕ is negative and it becomes dominant in the large L limit in (51).

3.2.2 Generalized conformal turbulence

Let us introduce the other possibilities that can be imposed on the conformal field theory. As we saw in section 2, there are many variants of the two-dimensional turbulence models where the enstrophy flow may depends on the viscosity. Also, the condition will be changed if one

have vanishing one point function which was originally considered by Polyakov. To get the corresponding object in the conformal turbulence, we need to compare the dissipation calculated by the viscosity term and nonlinear term in the Navier-Stokes equation. The correlation functions which we need to use is,

$$\begin{aligned} \langle \omega(z)\omega(0) \rangle &= L^{-2\Delta_\phi} |z|^{-4\Delta_\psi-4+2\Delta_\phi}. \\ \langle \omega(z)\delta_2\phi(0) \rangle &= L^{-2\Delta_\chi} |z|^{-2\Delta_\psi-2\Delta_\phi+2\Delta_\chi-6}. \end{aligned} \quad (52)$$

If we denote the short distance cutoff by δ , the dissipation rate of the enstrophy can be either computed as,

$$-\frac{d\Omega}{dt} = \eta \approx \nu \delta^{-6-4\Delta_\psi+2\Delta_\phi}, \quad (53)$$

by using the viscosity term, or can be alternatively given by,

$$-\frac{d\Omega}{dt} = \eta \approx \delta^{-6-2\Delta_\psi-2\Delta_\phi+2\Delta_\chi}, \quad (54)$$

by using the nonlinear term. In order to balance those two, we have to impose,

$$\nu \approx \delta^{2\Delta_\psi-4\Delta_\phi+2\Delta_\chi}. \quad (55)$$

The similar expression when we have vanishing one-point function is discussed by Hanany et. al.,

$$\nu \approx \delta^{2\Delta_\psi-2\Delta_\phi}. \quad (56)$$

By employing these relations, one may obtain the dependence of η on the viscosity as

$$\eta \approx \nu^{1-\gamma}, \quad \gamma = \gamma_1 = \frac{2\Delta_\psi - \Delta_\phi + 3}{\Delta_\psi - 2\Delta_\phi + \Delta_\chi}. \quad (57)$$

If we use the vanishing one-point function condition, γ_1 should be replaced by,

$$\gamma = \gamma_2 = \frac{2\Delta_\psi + 3}{\Delta_\psi - \Delta_\phi}. \quad (58)$$

In either case, if we employ the Kraichnan-Leith-Batchelor type condition, one has to impose,

$$\gamma_i = 1, \quad i = 1, 2, \quad (59)$$

and if we use Saffman type condition, we get,

$$\gamma_i = \frac{1}{3}, \quad i = 1, 2. \quad (60)$$

On the other hand, the parameter β defined in (19) may be expressed by the conformal dimensions as

$$\begin{aligned} \beta_i &= \frac{\gamma_i}{\alpha_i + 5}, \\ \beta_1 &= (2\Delta_\psi - 4\Delta_\phi + 2\Delta_\chi)^{-1}, \\ \beta_2 &= (2\Delta_\psi - 2\Delta_\phi)^{-1}, \end{aligned} \quad (61)$$

by comparing with (55-56). In this way, one can relate the dimensions of CFT primary fields with all the parameters which appeared in the previous section.

4 CFT models

In order to compute concrete values for the critical exponents, we need to solve (generalized) Polyakov's conditions (57) or (58) explicitly. This program is rather hard to be carried out analytically, hence, we have only solutions obtained from numerical computation. Previously, some of the CFT models of KLB type was found by [22] for vanishing one-point function case and by [6] for non-vanishing one point function case. In those papers, although CFT models are derived, the characteristic features which are common for those models are not discussed. In this paper, we study more extensive study for the generalized conditions (57) or (58) to get insights on the generic features of models which meet these conditions. We surveyed generalized Diofantian equations (59) (60) (we shall call them as P_i , and S_i (with $i = 1, 2$) in the following) up to $p < 1000$ and $q < 100$. As expected we got many CFT candidates, 1658 models for condition P1, 78 models for condition P2, 67 models for condition S1 and 75 models for condition S2. Later we prove that there are infinite number of solutions for any conditions of type (57).

Since we have several CFT models, we can not determine the exponents in the two dimensional turbulence uniquely. In figure 1a-d, we show the histogram of number of CFT models against the exponent of energy spectrum or each of the conditions. Where as in figure 1b,1d, we have rather flat spectrum in the range $-5 < \alpha < -3$, we have broader ($-5 < \alpha < 1$) and localized spectrum (peak located around $\alpha = -4.5, -3.5, -2.5, -1.5, -0.5, 0.5$) for the modified condition. We can also notice that a significant portion (82%) of the CFT models has their exponent in the range $-5 < \alpha < -4$.

We remark that in the course of computation, we need to determine operator ϕ as the lowest dimension operator in the OPE $\psi \times \psi$. By this process, we can classify the obtained models into two groups.

The first group, which we call category A below, is characterized by the fact that ϕ has already the dimension very close to the lowest dimension Δ_0 of the system. In this case, the dimension of χ is very close to ϕ since both of them are roughly same as Δ_0 . The situation remains same even if we take higher OPEs. Most of the solutions which we obtained belong to this category.

On the other hand, in the second class of solutions (category B), neither ϕ nor χ have dimension closer to Δ_0 . In this case, in every step we take OPE, we meet lower dimensional operator. Since Category B is simpler and can be classified completely, we start with it first.

4.1 Category B

The most interesting feature of solutions of this class is that we can find an infinite number of solutions for the condition of type (34) for *any fractional* γ . As far as we have observed, the solutions of those type always take the following form, i.e.

$$\begin{aligned} (p, q) &= (p_1(n-1)^2, q), \\ \psi &= (n, 1), \\ \phi &= (2n-1, 1), \\ \chi &= (3n-2, 1). \end{aligned} \tag{62}$$

It is obvious from (35) that there appears only primary fields of type $(r, 1)$ in the OPE of primary fields with index $s = 1$. On the other hand, the conformal dimension of fields $(r, 1)$ decreases as r increases as long as $r < p_1/q(n-1)^2$. One may confirm that ϕ is the minimum dimension in OPE $\psi \times \psi$ and so is χ in OPE $\psi \times \phi$ if

$$n > \frac{3y + 2 + \sqrt{9y^2 + 4y}}{2}, \quad y = q/p_1. \tag{63}$$

Also, for sufficiently large n , one may easily convince oneself that neither ϕ nor χ have dimension closer to the minimum dimension of the system.

Now if we put those combinations into (34), we get,

$$\eta \sim \nu^{1-\gamma} \quad \gamma \equiv \frac{2\Delta_\psi - \Delta_\phi + 3}{\Delta_\psi - 2\Delta_\phi + \Delta_\chi} = \frac{6p_1 - q}{q}. \tag{64}$$

The right hand side does not depend on n . For any fractional value for γ , we can adjust p_1 and q such that (64) can be satisfied. For example, to achieve KLB type condition ($\gamma = 1$), one may put

$$p_1 = 1, \quad q = 3. \tag{65}$$

For Saffman type condition ($\gamma = 1/3$), one may get,

$$p_1 = 2, \quad q = 9. \tag{66}$$

These give the solutions to the Diofantian equation for $n > 10$ in KLB case and for $n > 14$ for Saffman case. This simple observation shows that there are infinite number of solutions for the condition (34) for any γ .

One of the interesting feature of these solutions is that all of these models have same energy spectrum for each γ . Indeed, one may derive another cancellation of n ,

$$\alpha \equiv 4\Delta_\psi - 2\Delta_\phi + 1 = -\frac{q - p_1}{p_1}. \tag{67}$$

One can remove p_1 and q from relations (64) and (67),

$$\alpha = \frac{\gamma - 5}{\gamma + 1}. \quad (68)$$

The parameter β , on the other hand, can be similarly determined by,

$$\beta = \frac{\gamma}{\alpha + 5} = \frac{\gamma + 1}{6}. \quad (69)$$

For KLB, one has $(\alpha, \beta) = (-2, 1/3)$ and for Saffman type condition, one has $(\alpha, \beta) = (-7/2, 2/9)$. The latter model seems to fit rather well to the observed value for the energy spectrum $-4 < \alpha < -3$.

4.2 Category A

Although CFT models in category B has rather interesting properties, the majority (99%) of the solutions we obtained belong to this category. Although we can not solve the Diofantian equation in general, we can make several observations for this class.

Interestingly, the various exponents of the models in this class is (although approximately) related to the central charge of the system. The dependence itself is different for the conditions that we impose on the conformal models. If there are some methods where we can independently measure the central charge, one may judge which condition is the appropriate one.

In order to derive such formulae, it is essential to observe that

1. The operator product expansion of ψ field gives rise to a operator ϕ whose dimension is very close to the lowest dimension (Δ_0) of the system.
2. The central charge of the nonunitary minimal model is linearly related to Δ_0 .

To demonstrate the first fact, we make histograms of the difference of the conformal dimensions between field ϕ and Δ_0 (figure 2). We can see that deviation is less than 0.02. The second fact can be easily checked by recalling that $c = 1 - \frac{6(p-q)^2}{pq}$ and $\Delta_0 = \frac{1-(p-q)^2}{4pq}$. When p or q is sufficiently large, the first term in the denominator of Δ_0 may be neglected and one finds,

$$\Delta_0 = \frac{c - 1}{24}. \quad (70)$$

If we use the generalized condition (57), we get

$$\Delta_\psi = \frac{(1 - \gamma_1)\Delta_0 - 3}{2 - \gamma_1}. \quad (71)$$

The energy exponent may be then given by,

$$E(k) = k^{\alpha_1}, \quad \alpha_1 = \frac{-2\gamma_1\Delta_0 - \gamma_1 - 10}{2 - \gamma_1}. \quad (72)$$

In particular,

$$\alpha_1 = -11 - 2\Delta_0 \quad (\text{KLB}), \quad -8 - \Delta_0 \quad (\text{Saffman}). \quad (73)$$

Similarly, the viscous scale index β in (18) can be obtained as

$$\beta = \frac{\gamma_1 - 2}{2(\Delta_0 + 3)}, \quad (74)$$

for the condition (34). From the KLB and Saffman's condition, β reduces to

$$\beta = -\frac{1}{2(\Delta_0 + 3)} \quad (\text{KLB}), \quad -\frac{5}{6(\Delta_0 + 3)} \quad (\text{Saffman}). \quad (75)$$

Together with (70), it is clear that (72) gives the linear relation for the energy exponent and the central charge. We plot those relation in figure 3, to show that these are fulfilled rather nicely.

4.2.1 Families of infinite solutions in category A

Although the solutions of category A seem to occur randomly, there are several models that can be classified into several families of solutions. We would like to explain it by using the examples of condition P1.

First of all, as Chung et. al. has already pointed out, there are many occurrences of solutions (in our case, 1347 cases out of 1658), with special combination of primary fields,

$$\psi = (26, 2), \quad \phi = (15, 1), \quad \chi = (30, 2). \quad (76)$$

We would like to prove that this combination becomes the solution of conformal turbulence whenever

$$\frac{29}{2}q < p < \frac{31}{2}q, \quad (77)$$

with p and q coprime. Roughly speaking, this shows that there are q solutions of this type for each q . This fact explains quite systematic occurrence of solutions of this type.

The proof is quite elementary. We must first observe (76) solves (46) for arbitrary p and q . This requirement is equivalent to the algebraic equation

$$\begin{aligned} r_1^2 + r_2^2 - r_3^2 - 1 &= 0, \\ s_1^2 + s_2^2 - s_3^2 &= 0, \\ r_1 s_1 + r_2 s_2 - r_3 s_3 - 7 &= 0, \end{aligned} \quad (78)$$

if ψ, ϕ, χ are labeled (r_1, s_1) , (r_2, s_2) , and (r_3, s_3) .

The next step is to study when ϕ described in (76) becomes the lowest dimension operator in OPE. By explicitly comparing the dimension of ϕ with its neighbors, $(13, 1)$, $(17, 1)$, $(45, 3)$,

$(45, 5)$, $(47, 5)$, one finds that (77) is the desired condition. Under this condition, one can easily show that $\chi = (30, 2)$ is indeed the lowest dimension operator in OPE $\psi \times \phi$. (QED)

For this family of solutions, since the ratio of p and q is already given (77), one can determine the range of the exponents. For example, the range of α is immediately determined by using $\alpha = 3x + \frac{563}{x} - 87$,

$$-4.672 < \alpha < -4.177. \quad (79)$$

Since p can take arbitrary (of course, with coprime condition) integer value in (77), the distribution in this range is quite flat. This fact is quite consistent with figure 1a.

There are two other families of solutions with similar property, i.e. they satisfy (78). The first one is,

$$\psi = (55, 4), \quad \phi = (101, 7), \quad \chi = (115, 8), \quad (80)$$

and the second one is,

$$\psi = (362, 26), \quad \phi = (209, 15), \quad \chi = (418, 30). \quad (81)$$

There are 54 occurrence of the first family and 2 occurrence of the second one. One can similarly show that they contain infinite solutions as their member. The expected range of α is given by

$$\begin{aligned} -4.765 &< \alpha < -4.740, \\ -4.998 &< \alpha < -4.999, \end{aligned} \quad (82)$$

respectively.

Although 1418 of 1658 solutions are explainable in this way, there are still 240 solutions that we can not describe their origin. However, we may give some 'phenomenological' reasoning why there appear peaks around -3.5 , -2.5 , -1.5 , -0.5 , and 0.5 . As it turns out, those peaks comes from the models where ϕ happen to be $(17, 1)$, $(19, 1)$, $(21, 1)$, $(23, 1)$ and $(25, 1)$.² In order that those operators are roughly the lowest dimension fields, the ratio of $p/q = x$ should be $17, 19, 21, 23, 25$ respectively. Putting these values in (72), we get,

$$\alpha = -3.47, \quad -2.47, \quad -1.48, \quad -0.48, \quad -0.52, \quad (83)$$

respectively. Of these classification, there are 180 models.

To summarize, although CFT gives infinite number of solutions for Polyakov's criterion, we can extract quite a lot information from them. Especially, we can determine the relations between the exponents and have several models which have their α in the special range.

²We remark that the biggest peak around -4.5 comes from models with $\phi = (15, 1)$.

5 Higher Order Statistics

As we saw in the previous sections, the primary fields $\psi, \phi \dots$ are related to the observable in two dimensional turbulence through the energy exponent. Now some natural question arises. In general, there are many other primary fields in the minimal models. How can we extract some informations for those fields? Here we propose that one direction we may take is to go further to calculate higher correlation functions. As long as the assumption of the local equilibrium is correct, if one makes the dimensionless combination such as, $\langle \psi^3 \rangle / \langle \psi^2 \rangle^{3/2}$, it should be a dimensionless constant and there should be no dependence on the Reynolds number. In CFT, this is not true because there are singularities in the short distance expansion.

In the correlation function, $\langle \psi \psi \dots \psi \rangle$, the dominant contribution comes from the one point function of the lowest dimension in the OPE $[\psi] \times [\psi] \dots [\psi]$. This gives the L dependence of the correlation function. On the other hand, the singularity coming from the short distance expansion of ψ fields can be expressed as power of the short distance cutoff δ . Let us denote ϕ_n as the lowest dimension operator in the n th order product and Δ_n as the dimension of ϕ_n . We may evaluate the n point function in terms of them,

$$\langle \psi^n \rangle \sim L^{-2\Delta_n} \delta^{-2n\Delta_\psi + 2\Delta_n}. \quad (84)$$

It follows that the non-trivial dependence on δ for the dimensionless combination,

$$F_n = \frac{\langle \psi^n \rangle}{\langle \psi^2 \rangle^{n/2}} \sim (L/\delta)^{-2\Delta_n + n\Delta_\phi} \sim Re^{\beta_n}. \quad (85)$$

Here β_n is the exponent for n th order products:

$$\beta_n \equiv -\beta(2\Delta_n - n\Delta_\phi). \quad (86)$$

The simplest choice F_3 and F_4 corresponds to what is usually called “skewness” and “flatness” in the fluid dynamics community. We shall denote the exponents for $n = 3, 4$ as β_S and β_F in the following discussions.

5.1 Category A

For this category, one may substitute $\Delta_n = \Delta_0$ in (86). Using (75), one obtains

$$\begin{aligned} \beta_k &= -\beta(2\Delta_k - k\Delta_\phi) \\ &= \frac{\Delta_0(k-2)(\gamma-2)}{2(3+\Delta_0)}. \end{aligned} \quad (87)$$

5.2 Category B

Skewness and Flatness may be computed by using, $\Delta_3 = \Delta_\chi$ and $\Delta_4 = \Delta_{(4n-3,1)}$, which is valid for $n > 2y + 1 + \sqrt{4y^2 + y}$. Amazingly, even the dependence on parameter γ disappears.

$$\begin{aligned}\beta_S &\equiv -\beta(2\Delta_\chi - 3\Delta_\phi) = -\frac{3}{2}, \\ \beta_F &\equiv -\beta(2\Delta_4 - 4\Delta_\phi) = -4.\end{aligned}\tag{88}$$

In general, if the minimum dimension operator in k th product of ψ is given by $(kn - k + 1, 1)$, the k th exponent is

$$\beta_k = \frac{k(2 - k)}{2}.\tag{89}$$

In this way, we find that the solutions for category B gives *unique* prediction for the higher exponents.

6 Casimir Invariants

Up to now, CFT is supposed to describe the time independent aspect of the two dimensional turbulence. However, the use of Navier-Stokes equation gives a simple explanation time dependence for the decaying turbulence³. In particular, we would like to discuss the decay rate of Casimir invariants Ω_n in detail to compare the results from CFT to our numerical computation. One may easily find it as,

$$\eta_n = \frac{n(n-1)\nu}{2} <\omega^{n-2}(\nabla\omega)^2> \propto \nu \delta^{2\Delta_n - 2n\Delta_\psi - 2n-2} L^{-2\Delta_n}.\tag{90}$$

As usual, Δ_n is the minimum dimension in the OPE of n ψ fields. On the other hand, a dimensional argument shows

$$\eta_n = \frac{\nu}{\delta^2} \Omega^{\frac{n}{2}} \left(\frac{L}{\delta}\right)^{\alpha_n},\tag{91}$$

where α_n denotes an anomalous dimension for η_n . Comparing (90) and (91), we find

$$\alpha_n = 2n(\Delta_\psi + 1) - 2\Delta_n.\tag{92}$$

Using (10), (18) and (92), (91) becomes

$$\eta_n = \Omega^{\frac{n}{2}\{-\beta(\Delta_\psi+1)+1\}+1-\beta(\Delta_n+1)} \left(\frac{E}{\nu}\right)^{2\beta(\Delta_\psi+1)n-2\beta(\Delta_n-1)-1}.\tag{93}$$

³ This process seems to be similar to the deformation of conformal field theory by coupling the relevant operators to conformal invariant system discussed by Zamolodchikov[31]. In his discussion, the central charge c behaves as the Morse function in the theory space of CFT and increases its value in the process of renormalization group. In order to apply his argument to turbulence, we need to extend his argument to include the non-unitary theory. We would like to discuss this aspect in future issues.

Substituting (26) into (93), we can estimate the decay rate of Ω_n as

$$\eta_n \propto \left(\frac{\nu}{E}\right)^{p_n} t^{q_n}, \quad (94)$$

where the powers p_n and q_n can be obtained as

$$\begin{aligned} p_n &= \frac{2\beta(\Delta_\psi + 1) + 1 - \gamma}{\gamma - 2} n + \frac{2\beta(1 - \Delta_n) - \gamma}{\gamma - 2}, \\ q_n &= \frac{\beta(-2\Delta_\psi + 1) + 1}{\gamma - 2} n + \frac{-2\beta(1 - \Delta_n) + 2}{\gamma - 2}. \end{aligned} \quad (95)$$

On the other hand, the random phase approximation described in section 2 leads to

$$p_n = (1 - \gamma)(1 + \frac{n}{\gamma - 2}), \quad (96)$$

$$q_n = -1 + \frac{n}{\gamma - 2}. \quad (97)$$

We can see that this difference originates in the anomalous dimension.

6.1 Category A

Using (95), (71) and (74), the exponents p_n , q_n of decay rate can be obtained as

$$\begin{aligned} p_n &= -\frac{2}{\Delta_0 + 3} n + \frac{2\{-\gamma_1(\Delta_0 + 1) + \Delta_0 - 1\}}{(\Delta_0 + 3)(\gamma_1 - 2)}, \\ q_n &= -\frac{\Delta_0 + 1}{\Delta_0 + 3} n + \frac{\gamma_1(\Delta_0 - 1) + 8}{(\Delta_0 + 3)(\gamma_1 - 2)}. \end{aligned} \quad (98)$$

They become

$$\begin{aligned} p_n &= -\frac{2(n - 2)}{\Delta_0 + 3}, \\ q_n &= -\frac{(\Delta_0 + 1)n + \Delta_0 + 7}{\Delta_0 + 3}, \end{aligned} \quad (99)$$

for the KLB condition and

$$\begin{aligned} p_n &= -\frac{10n + 4(\Delta_0 - 2)}{\Delta_0 + 3}, \\ q_n &= -\frac{5(\Delta_0 + 1)n + \Delta_0 + 23}{\Delta_0 + 3}, \end{aligned} \quad (100)$$

for the Saffman condition.

6.2 Category B

The decay rate for the higher Casimir invariant can be found from (69). After some computation, we get

$$\begin{aligned} p_n &= \frac{1}{2(\gamma+1)}n^2 - \frac{8\gamma^2 + \gamma - 16}{6(\gamma+1)(\gamma-2)}n - \frac{2(2\gamma-1)}{3(\gamma-2)}, \\ q_n &= -\frac{1}{2(\gamma+1)}n^2 + \frac{2\gamma^2 + 7\gamma - 4}{6(\gamma+1)(\gamma-2)} + \frac{4+\gamma}{3(\gamma-2)}. \end{aligned} \quad (101)$$

Unlike category A, these exponents grows as n^2 . They become

$$\begin{aligned} p_n &= \frac{1}{4}n^2 - \frac{7}{12}n + \frac{2}{3}, \\ q_n &= \frac{-1}{4}n^2 - \frac{5}{12}n - \frac{5}{3}, \end{aligned} \quad (102)$$

for the KLB condition and,

$$\begin{aligned} p_n &= \frac{3}{8}n^2 - \frac{133}{120}n - \frac{2}{15}, \\ q_n &= -\frac{3}{8}n^2 + \frac{13}{120}n - \frac{13}{15}, \end{aligned} \quad (103)$$

for the Saffman condition.

7 Numerical Analysis

In this section, some statistical properties predicted by CFT are compared with the numerical data obtained by the direct simulation. The pseudospectral method is used, which efficiently computes convolutions of the nonlinear terms in the physical space and is fully dealiased by the two-third law. The modes are 256×256 , the time integration is performed by the second-order Runge-Kutta scheme up to $t = 10$ and the width for time step is 0.002. We examined five different cases of viscosity, $\nu = 0.0001, 0.0003, 0.001, 0.003$ and 0.01 and main results for the first four cases are shown. Decaying turbulence created by (1) without external forcing is investigated.

Temporal evolution of energy E , enstrophy Ω and enstrophy dissipation rate η is shown in Figures 4a-c. Initial increase of η is observed until $t \approx 5$ for $\nu = 0.0001$ and the decay of Ω and η is prominent after $t = 7$. Thus, data in the time interval $7 \leq t \leq 10$ are used to fit the asymptotic behavior of η :

$$\eta \propto (\nu/E)^p(t + t_0)^q, \quad (104)$$

where t in (27) is replaced by $t + t_0$ in order to get a more precise power from the finite-time integration. The time offset t_0 is estimated by the asymptotic expression of $\Omega/\eta \approx a(t + t_0)$,

which is independent of q and the data $7 \leq t \leq 10$. Numerically obtained values of parameters in (104) are shown in Table 2.

Although the numerical power of t varies from -4 to -2.2 according to ν , it is nearly constant when $0.001 \leq \nu \leq 0.003$, which is obtained by the proper resolution and closer to that of Saffman than that of Batchelor. (See the energy spectrum in Figure 4d) The power p is obtained as -0.171 by the two cases $\nu = 0.001, 0.003$ and the energy averaged in the time interval $7 \leq t \leq 10$, which is close to but slightly larger than Saffman's value -0.133 . Comparing (104) with (27), relations between p, q and γ are obtained as

$$p = \frac{\gamma(1 - \gamma)}{\gamma - 2}, \quad (105)$$

$$q = \frac{4 - \gamma}{\gamma - 2}. \quad (106)$$

Although γ varies from 0.333 to 1.333 from the numerical data of q , the plausible value of $p = -0.171$ leads to $\gamma = 0.614$ or 0.557 . From (22) we obtain $\eta \approx \nu^{1-\gamma}$ and the power lies between 0.386 to 0.443 . The obtained power locates between the KLB value 0 and the Saffman's value $2/3$.

The temporal evolution of the inviscid invariant Ω_n and its dissipation rate η_n is examined and shown in Figures 5a,b for $\nu = 0.0003$ and even n between 4 and 20 . For odd n , Ω_n oscillates irregularly around zero and no clear dependence on ν or n is observed. The adopted numerical method does not conserve Ω_n even if $\nu = 0$ because of truncation in the Fourier space, although energy and enstrophy are conserved. In fact, oscillations appear in Ω_n in the case of the smallest viscosity and large n . However, we analyze the data of η_n since the deviation is not monotonic and the decay dominates the oscillation for the most cases.

Similar to the η , the following asymptotic form of η_n for even n is assumed:

$$\eta_n \propto (\nu/E)^{p_n} (t + t_0)^{q_n}. \quad (107)$$

Figure 3a shows the powers q_n versus n for the four cases. If there is an n dependence of q_n predicted by conformal field theory like

$$q_n = q_0 + nq_1, \quad (108)$$

we may estimate them by the data shown in Figure 7. Table 3 shows estimated values of q_0 and q_1 . Constants q_0 are within the values of (99) or (100) predicted by category A. However, for q_1 , numerical values are smaller than theoretical ones.

The other parameter p_n , denoted by

$$p_n = p_0 + np_1, \quad (109)$$

is also estimated by plotting $\log C_n / \log(\nu/E)$ where C_n is $\eta_n / (t + t_0)^{q_n}$. We find negative values, between -0.422 and -0.265, of p_0 and, between -0.0145 and -0.00525, of p_1 the latter is very small. Since the constants C_n include a constant proportional to n^2 , the degree of coincidence is unsatisfactory.

For skewness and flatness, we should determine what kind of variables is to be measured. We choose

$$S = -\frac{2 \langle u_x \omega_x^2 \rangle}{\langle u_x^2 \rangle^{1/2} \langle \omega_x^2 \rangle} \quad (110)$$

and

$$F = \frac{\langle \omega_x^4 \rangle}{\langle \omega_x^2 \rangle^2} \quad (111)$$

since they show rapid growth in the initial stage $t \approx 2$. The former is related with production of palinstrophy. In Figure 7a,b maxima of S and F versus ν at the initial increase are plotted. We observe that both S and F increases as ν decreases, as is observed in many experiments of three-dimensional turbulence [30]. Intermittency of turbulence is responsible for the tendency that skewness and flatness increase as Reynolds number becomes large. We observe that $S \approx Re^{0.117}$ and $F \approx Re^{0.222}$. On the other hand, the predicted feature for S and F is the opposite, i.e., the decreases as Reynolds number increases. Actually this prediction contradicts with observations so far. Since the behaviour of higher order statistics is strongly dependent on what is the measured physical quantity, there may exist observables faithful to the present prediction.

8 Conclusions and Discussions

It is shown that the extended theory of two-dimensional turbulence characterized by the energy exponent and the viscous scale index can clarify relations between classical and conformal field theories. New classes of CFT solutions for two-dimensional turbulence are obtained and its statistical predictions are explored. Many of the obtained exponents of the energy spectrum lie between or close to the reliable values -3 and -4 . The dependence of Casimir invariants on the energy, enstrophy and viscosity is shown and used to predict its decay rate. Dependence of skewness and flatness on Reynolds number are also revealed and the predicted tendency is contrary to intermittency effects in three-dimensional turbulence. This may imply that the quantities to be measured are not the usual ones like $\partial\omega/\partial x$.

There are some possibilities for further study of higher order quantities. For flatness, behaviors of other quantities, e.g., ψ , ω , can be investigated if the integration time is so large that isolated coherent vortices emerge. To perform more precise numerical investigation on $\langle \omega^n \rangle$, we can invoke the Zeitlin's finite-mode system, which was studied numerically in detail by Hattori [13]

without viscosity. In this system the efficient FFT method is not available and its simulation requires much CPU time for integration.

9 Acknowledgements

Numerical simulation was performed by IBM RS/6000 workstations in International Center for Elementary Particle Physics, University of Tokyo, which are supplied for a partnership program with IBM Japan, ltd. This work is also supported by Grant-in-Aid for Scientific Research from the Ministry of Education, Science and Culture in Japan.

10 Figure Captions

Figure 1. Histogram of the CFT solutions versus energy exponent, by using KLB condition (a), and Saffman condition (b). In both of the case, we assume that the one point function is not vanishing.

Figure 2. Histograms of the difference between the dimension of ϕ and the lowest dimension of the system. We use KLB condition (a) and Saffman condition (b). Here we removed datum of category B.

Figure 3. Relation between the central charge and and energy exponent. We use KLB condition (a) and Saffman condition (b).

Figure 4. Temporal evolution of the energy (a), enstrophy (b) and enstrophy dissipation rate (c) and energy spectrum (d) at $t = 10$. Four cases with the viscosity $\nu = 0.0001, 0.0003, 0.001, 0.003$ are drawn by solid, dashed, dotted and dot-dashed lines. A dashed straight line in (d) shows the k^{-4} energy spectrum.

Figure 5. Temporal evolution of Ω_n (a) and η_n (b) for the case $\nu = 0.0003$. Values for $n = 4, 6, 8, \dots, 20$ are denoted in the order from below.

Figure 6. Numerically obtained values of the powers q_n in (108). Cases $\nu = 0.0001, 0.0003, 0.001, 0.003$ are denoted by a circle, square, diamond and cross respectively.

Figure 7. Numerically obtained maxima in the initial growth of skewness (a) and flatness (b) defined in (110) and in (111) versus Re .

11 Table Captions

Table 1. First few solutions for CFT turbulence. (a) KLB condition (with non-vanishing one-point function)

(p,q)	ψ	ϕ	χ	α
(33,2)	$\Delta_{10,1} \sim -3.00$	$\Delta_{17,1} \sim -3.64$	$\Delta_{16,1} \sim -3.64$	-3.73
(43,3)	$\Delta_{12,1} \sim -3.01$	$\Delta_{15,1} \sim -3.09$	$\Delta_{14,1} \sim -3.10$	-4.84
(44,3)	$\Delta_{18,1} \sim -2.99$	$\Delta_{15,1} \sim -3.18$	$\Delta_{14,1} \sim -3.18$	-4.61
(46,3)	$\Delta_{20,1} \sim -2.99$	$\Delta_{15,1} \sim -3.35$	$\Delta_{16,1} \sim -3.34$	-4.28
(52,3)	$\Delta_{25,1} \sim -3.00$	$\Delta_{17,1} \sim -3.85$	$\Delta_{17,1} \sim -3.85$	-3.31
(67,3)	$\Delta_{36,1} \sim -3.00$	$\Delta_{23,1} \sim -5.09$	$\Delta_{22,1} \sim -5.09$	-0.84
(77,3)	$\Delta_{43,1} \sim -3.00$	$\Delta_{25,1} \sim -5.92$	$\Delta_{25,1} \sim -5.92$	0.84
(100,3)	$\Delta_{11,1} \sim -4.10$	$\Delta_{21,1} \sim -6.70$	$\Delta_{31,1} \sim -7.80$	-2.00
(121,3)	$\Delta_{12,1} \sim -4.61$	$\Delta_{23,1} \sim -7.73$	$\Delta_{34,1} \sim -9.34$	-2.00

(b) Saffman condition (with non-vanishing one-point function)

(p,q)	ψ	ϕ	χ	α
(97,4)	$\Delta_{12,1} \sim -4.03$	$\Delta_{23,1} \sim -5.56$	$\Delta_{24,1} \sim -5.57$	-3.99
(74,5)	$\Delta_{12,1} \sim -3.08$	$\Delta_{15,1} \sim -3.22$	$\Delta_{14,1} \sim -3.21$	-4.91
(86,5)	$\Delta_{23,1} \sim -3.33$	$\Delta_{17,1} \sim -3.81$	$\Delta_{17,1} \sim -3.81$	-4.67
(139,5)	$\Delta_{43,1} \sim -4.38$	$\Delta_{27,1} \sim -6.45$	$\Delta_{27,1} \sim -6.45$	-3.62
(284,5)	$\Delta_{95,1} \sim -7.28$	$\Delta_{57,1} \sim -13.70$	$\Delta_{57,1} \sim -13.70$	-0.72
(131,6)	$\Delta_{32,1} \sim -3.79$	$\Delta_{21,1} \sim -4.96$	$\Delta_{22,1} \sim -4.97$	-4.22
(117,7)	$\Delta_{22,1} \sim -3.28$	$\Delta_{17,1} \sim -3.69$	$\Delta_{16,1} \sim -3.69$	-4.72
(299,8)	$\Delta_{14,1} \sim -5.20$	$\Delta_{27,1} \sim -8.13$	$\Delta_{38,1} \sim -8.85$	-3.52
(196,9)	$\Delta_{77,4} \sim -3.78$	$\Delta_{109,5} \sim -4.96$	$\Delta_{87,4} \sim -4.96$	-4.22

(c) KLB condition (with vanishing one-point function)

(p,q)	ψ	ϕ	χ	α
(21,2)	$\Delta_{4,1} \sim -1.14$	$\Delta_{7,1} \sim -1.86$	$\Delta_{10,1} \sim -2.14$	-3.57
(25,3)	$\Delta_{11,1} \sim -1.40$	$\Delta_{9,1} \sim -1.60$	$\Delta_{9,1} \sim -1.60$	-4.60
(26,3)	$\Delta_{5,1} \sim -1.31$	$\Delta_{9,1} \sim -1.69$	$\Delta_{9,1} \sim -1.69$	-4.23
(55,6)	$\Delta_{14,1} \sim -1.18$	$\Delta_{9,1} \sim -1.82$	$\Delta_{10,1} \sim -1.80$	-3.73
(62,7)	$\Delta_{13,1} \sim -1.26$	$\Delta_{9,1} \sim -1.74$	$\Delta_{9,1} \sim -1.74$	-4.03
(67,8)	$\Delta_{28,3} \sim -1.38$	$\Delta_{25,3} \sim -1.62$	$\Delta_{42,5} \sim -1.62$	-4.51
(71,9)	$\Delta_{32,4} \sim -1.50$	$\Delta_{55,7} \sim -1.50$	$\Delta_{32,4} \sim -1.50$	-4.99
(87,11)	$\Delta_{16,2} \sim -1.51$	$\Delta_{23,3} \sim -1.49$	$\Delta_{16,2} \sim -1.51$	-5.03
(91,11)	$\Delta_{14,2} \sim -1.40$	$\Delta_{25,3} \sim -1.60$	$\Delta_{16,2} \sim -1.59$	-4.61

(d) Saffman condition (with vanishing one-point function)

(p,q)	ψ	ϕ	χ	α
(17,2)	$\Delta_{6,1} \sim -1.47$	$\Delta_{9,1} \sim -1.65$	$\Delta_{8,1} \sim -1.65$	-4.88
(41,2)	$\Delta_{4,1} \sim -1.32$	$\Delta_{7,1} \sim -2.41$	$\Delta_{10,1} \sim -3.29$	-4.27
(46,3)	$\Delta_{27,1} \sim -1.13$	$\Delta_{15,1} \sim -3.35$	$\Delta_{15,1} \sim -3.35$	-3.52
(46,5)	$\Delta_{13,1} \sim -1.43$	$\Delta_{9,1} \sim -1.83$	$\Delta_{9,1} \sim -1.83$	-4.74
(53,6)	$\Delta_{12,1} \sim -1.45$	$\Delta_{9,1} \sim -1.74$	$\Delta_{8,1} \sim -1.72$	-4.81
(65,6)	$\Delta_{17,1} \sim -1.35$	$\Delta_{11,1} \sim -2.23$	$\Delta_{11,1} \sim -2.23$	-4.42
(91,8)	$\Delta_{41,3} \sim -1.33$	$\Delta_{57,5} \sim -2.37$	$\Delta_{57,5} \sim -2.37$	-4.31
(131,8)	$\Delta_{62,3} \sim -1.08$	$\Delta_{49,3} \sim -3.61$	$\Delta_{82,5} \sim -3.61$	-3.31
(79,10)	$\Delta_{39,5} \sim -1.50$	$\Delta_{71,9} \sim -1.51$	$\Delta_{39,5} \sim -1.50$	-4.99

Table 2. Numerically obtained values of the time offset t_0 , the power q in (104) and γ in (106).

ν	t_0	q	γ
0.0001	24.3	-4.03	1.34
0.0003	16.8	-3.61	1.23
0.001	3.58	-2.28	0.438
0.003	1.21	-2.36	0.529

Table 3. Numerically obtained values of the constants q_0 and q_1 in (108).

ν	q_0 ($4 \leq n \leq 20$)	q_1 ($4 \leq n \leq 20$)	q_0 ($12 \leq n \leq 20$)	q_1 ($12 \leq n \leq 20$)
0.0001	-7.41	-0.326	-8.64	-0.245
0.0003	-5.84	-0.0997	-3.43	-0.245
0.001	-2.95	-0.126	-1.35	-0.225
0.003	-1.86	-0.451	-1.05	-0.503

References

- [1] G. K. Batchelor, Computation of the energy spectrum in homogeneous two-dimensional turbulence, *Phys. Fluids Suppl.*, II 12 (1969) 233-239.
- [2] A. A. Belavin, A. M. Polyakov and A. B. Zamolodchikov, *J. Stat. Phys.* 34 (1984) 763, *Nucl. Phys.* B241 (1984) 333;
- [3] M. E. Brachet, M. Meneguzzi, H. Politano and P. L. Sulem, The dynamics of freely decaying two-dimensional turbulence *J. Fluid Mech.* 194 (1988) 333-349.
- [4] J.L. Cardy, Conformal Invariance and the Yang-Lee edge singularity in two dimensions, *Phys. Rev. Lett.* 54 (1985) 1354;
- [5] B. K. Chung, S. Nam, Q. -H. Park and H. J. Shin, Conformal turbulence with boundary, *Phys. Lett.* 309B (1993) 58; Possible tests of conformal turbulence through boundaries, KHTP-93-08, SNUCTP-93-38 (1993).
- [6] B. K. Chung, S. Nam, Q. -H. Park and H. J. Shin, Solutions of conformal turbulence on a half plane, KHTP-93-07/SNUCTP-93-37 (1993).
- [7] M.E. Fisher, Yang-Lee edge singularity and ϕ^3 field theory, *Phys. Rev. Lett.* 40 (1978) 1610.
- [8] G. Falkovich and A. Hanany, Spectra of conformal turbulence, Preprint WIS-92-88-PH, hep-th/9212015 (1992).
- [9] G. Falkovich and A. Hanany, Is 2d Turbulence a conformal turbulence? Preprint WIS-93-5 PH, hep-th/9301030. 1993
- [10] P. Di Francesco, H. Saleur and J.B. Zuber, Critical Ising correlation functions in the plane and on the torus, *Nucl. Phys.* B290 (1987) 527.
- [11] G. Ferretti and Z. Yang, Magnetic fields and passive scalars in Polyakov's conformal turbulence, *Europhys. Lett.* 22 (1993) 639.
- [12] A. D. Gilbert, Spiral structures and spectra in two-dimensional turbulence, *J. Fluid Mech.* 193 (1988) 475-497.
- [13] Y. Hattori, Effect of phase dependent invariants and ergodicity in finite-mode systems closely related with two-dimensional ideal flow, *J. Phys. Soc. Jpn.* 62 (1993) 2293-2305.
- [14] J. R. Herring, S. A. Orszag, R. H. Kraichnan and D. G. Fox Decay of two-dimensional homogeneous turbulence, *J. Fluid Mech.* 66 (1974) 417-444.

- [15] C. Itzykson and J-M. Drouffe, Statistical field theory, Chap.9, (Cambridge, 1989).
- [16] S. Kida, Numerical simulation of two-dimensional turbulence with high-symmetry, *J. Phys Soc. Jpn.* 54 (1985) 2840-2845.
- [17] R. H. Kraichnan, Inertial ranges in two dimensional turbulence *Phys Fluids* 10 (1967) 1417-1423.
- [18] R. H. Kraichnan, Inertial-range transfer in two- and three-dimensional turbulence *J. Fluid Mech.* 47 (1971) 525-535.
- [19] A. N. Kolmogorov, The local structure of turbulence in incompressible viscous fluid for very large Reynolds numbers, *Dokl. Akad. Nauk SSSR* 30 (1941) 301-305.
- [20] C. E. Leith, Diffusion approximation for two dimensional turbulence, *Phys. Fluids* 11 (1968) 671-673.
- [21] D. A. Lowe, Conformal models of two-dimensional turbulence, *Mod. Phys. Lett. A8* (1993) 923.
- [22] Y. Matsuo, Some additional solutions of conformal turbulence, *Mod. Phys. Lett. A8* (1993) 619.
- [23] J. C. McWilliams, The emergence of isolated coherent vortices in turbulent flow, *J. Fluid Mech.* 146 (1984) 21-43.
- [24] D. Montgomery and G. Joyce, Statistical mechanics of "negative temperature" states, *Phys. Fluids* 17 (1974) 1139-1145.
- [25] D. Montgomery, W. H. Matthaeus, W. T. Stribling, D. Martinez and S. Oughton, Relaxation in two dimensions and the "sinh-Poisson" equation, *Phys. Fluids* A4 (1992) 3-6.; D. Montgomery, X. Shan and W. H. Matthaeus, Navier-Stokes relaxation to sinh-Poisson states at finite Reynolds numbers, *Phys. Fluids* A5 (1993) 2207-2216.
- [26] A. M. Polyakov, Conformal turbulence, Princeton Preprint PUPT-1341, hep-th/9209046 (1992).
- [27] A. M. Polyakov, The theory of turbulence in two dimensions, *Nucl. Phys. B396* (1993) 367.
- [28] P. G. Saffman, On the spectrum and decay of random two-dimensional vorticity distributions of large Reynolds number *Stud. Appl. Math.* 50 (1971) 377-383.

- [29] P. Santangelo, R. Benzi and B. Legras, The generation of vortices in high-resolution, two-dimensional decaying turbulence and the influence of initial conditions on the breaking of self-similarity, *Phys. Fluids A1* (1989) 1027-1034.
- [30] C. W. Van Atta and R. A. Antonia, Reynolds number dependence of skewness and flatness factors of turbulent velocity derivatives. *Phys. Fluids* 23 (1980) 252-257.
- [31] A. B. Zamolodchikov, *JETP Letters* 43 (1986) 730; See also C. Itzykson and H. Saleur, *J. Stat. Phys.* 48 (1987) 449.
- [32] V. Zeitlin, Finite-mode analogs of 2D ideal hydrodynamics: Coadjoint orbits and local canonical structure, *Physica D49* (1991) 353-362.

Figure 1 (a)

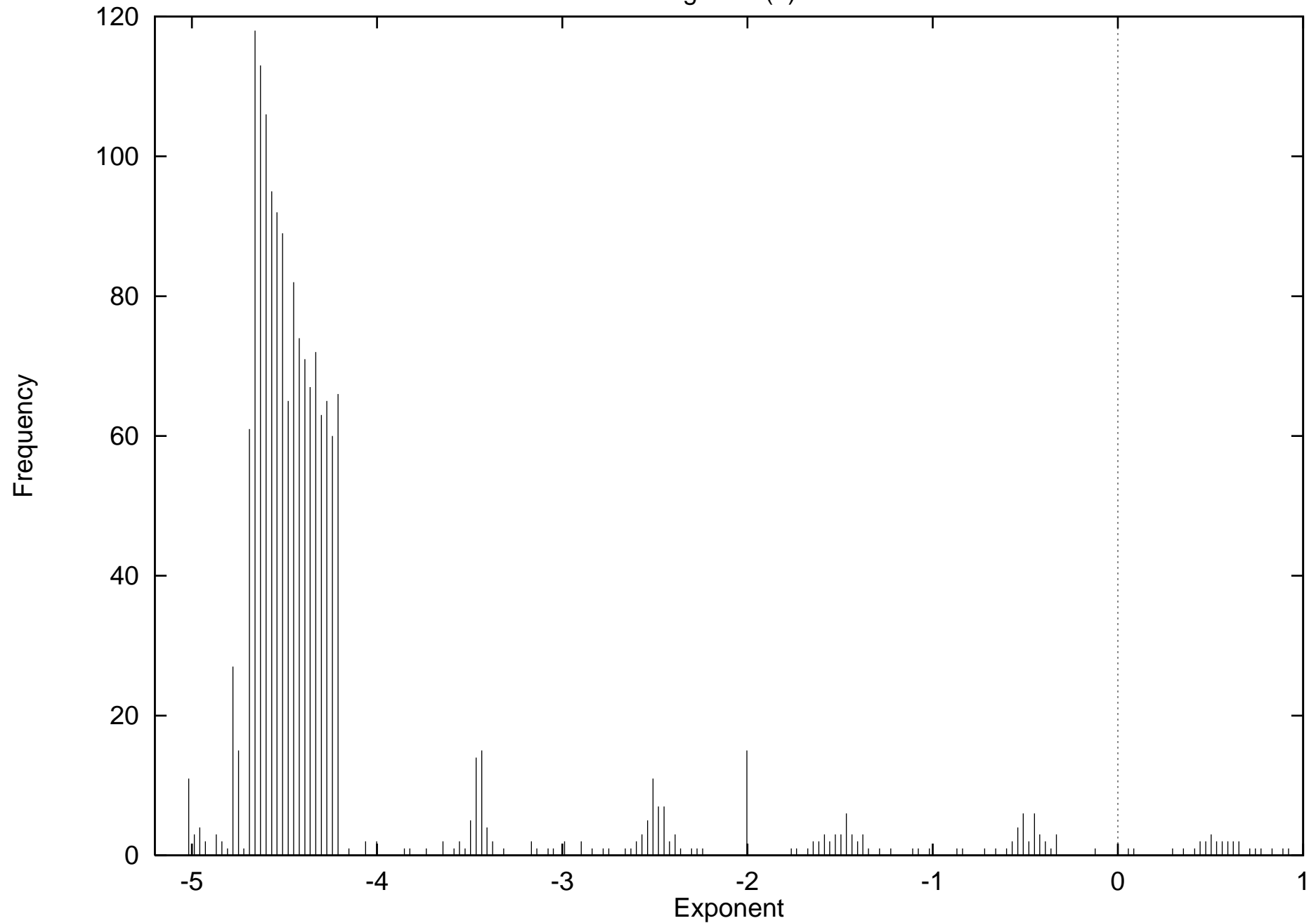


Figure 1 (b)

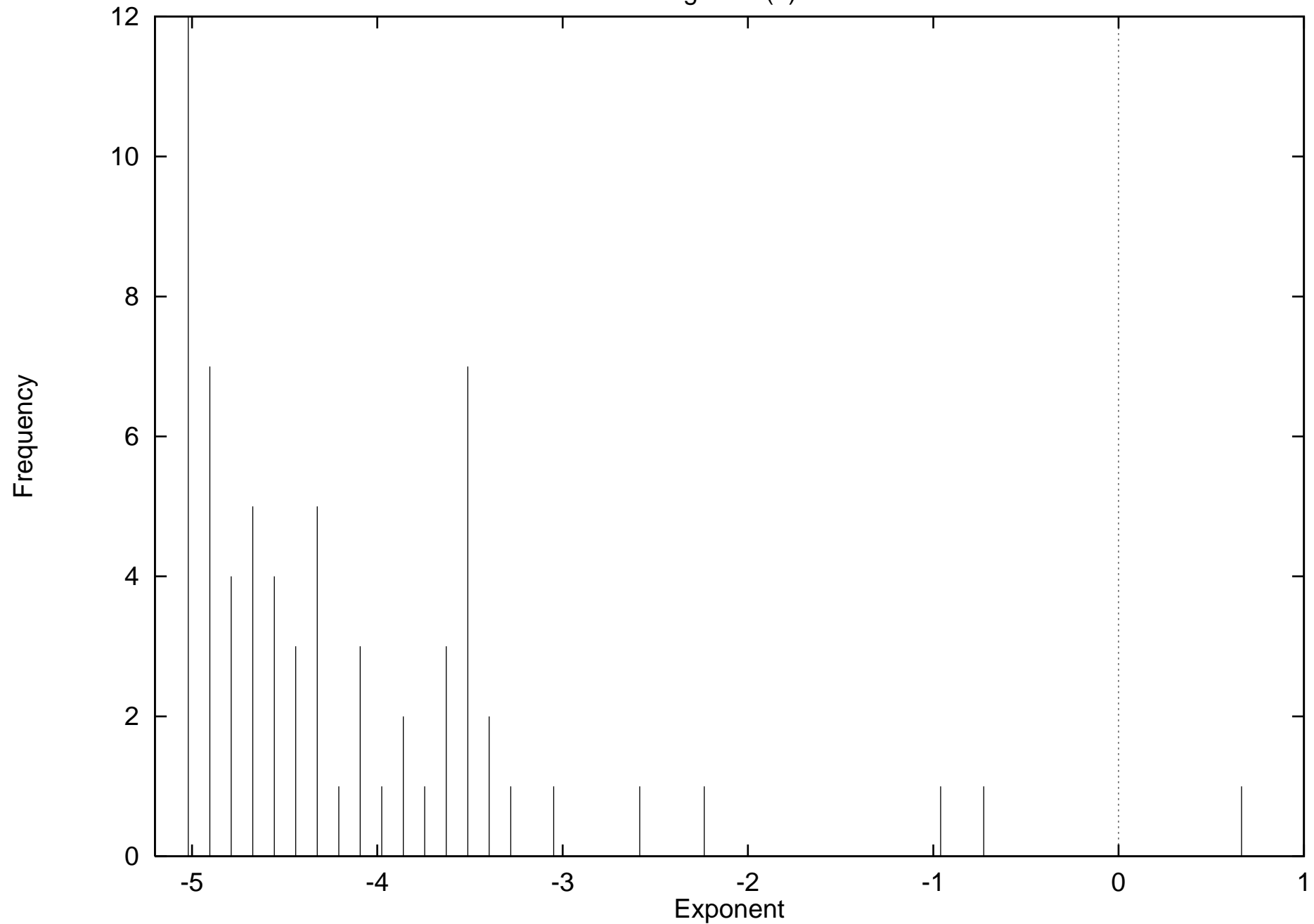


Figure 2 (a)

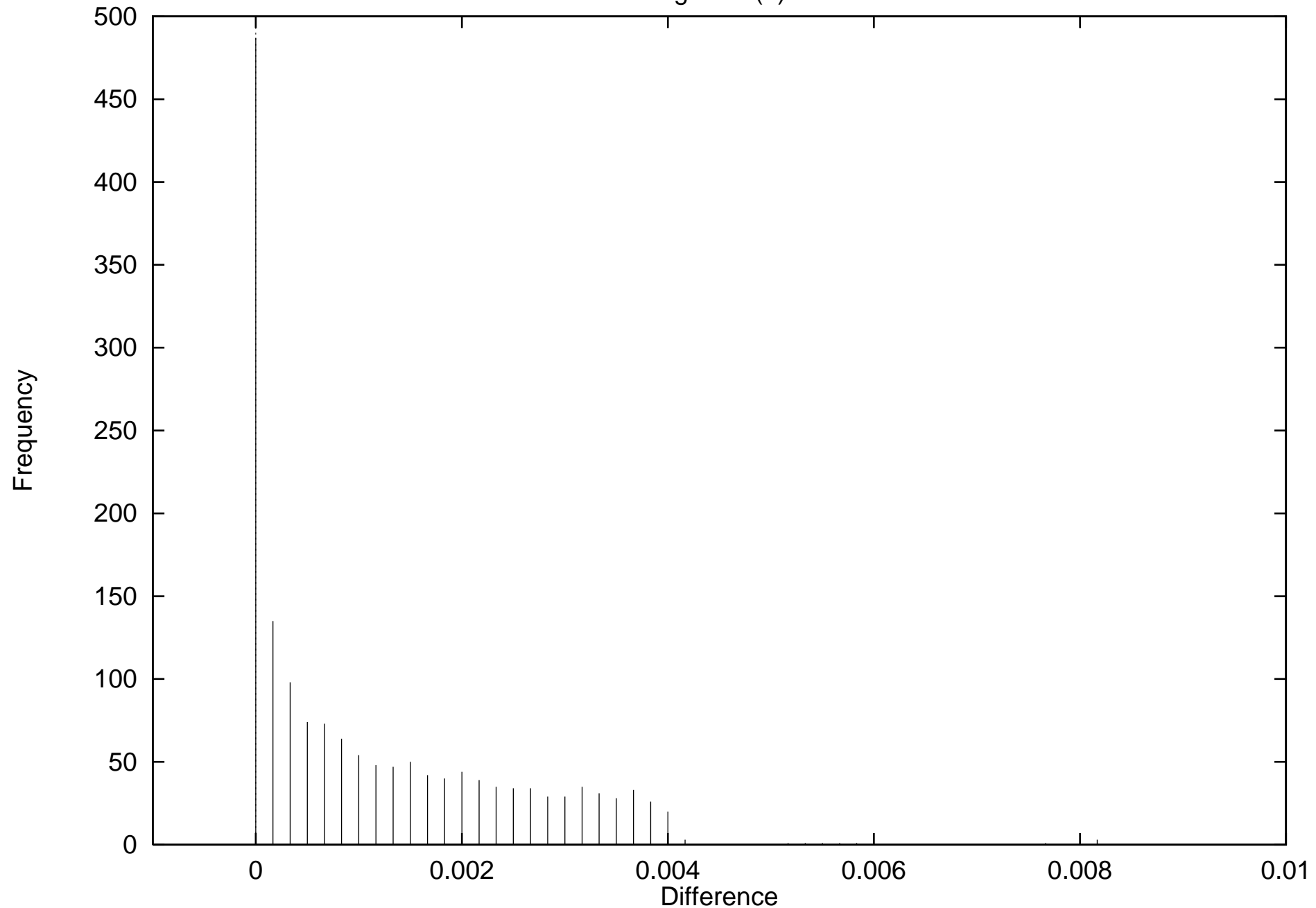


Figure 2 (b)

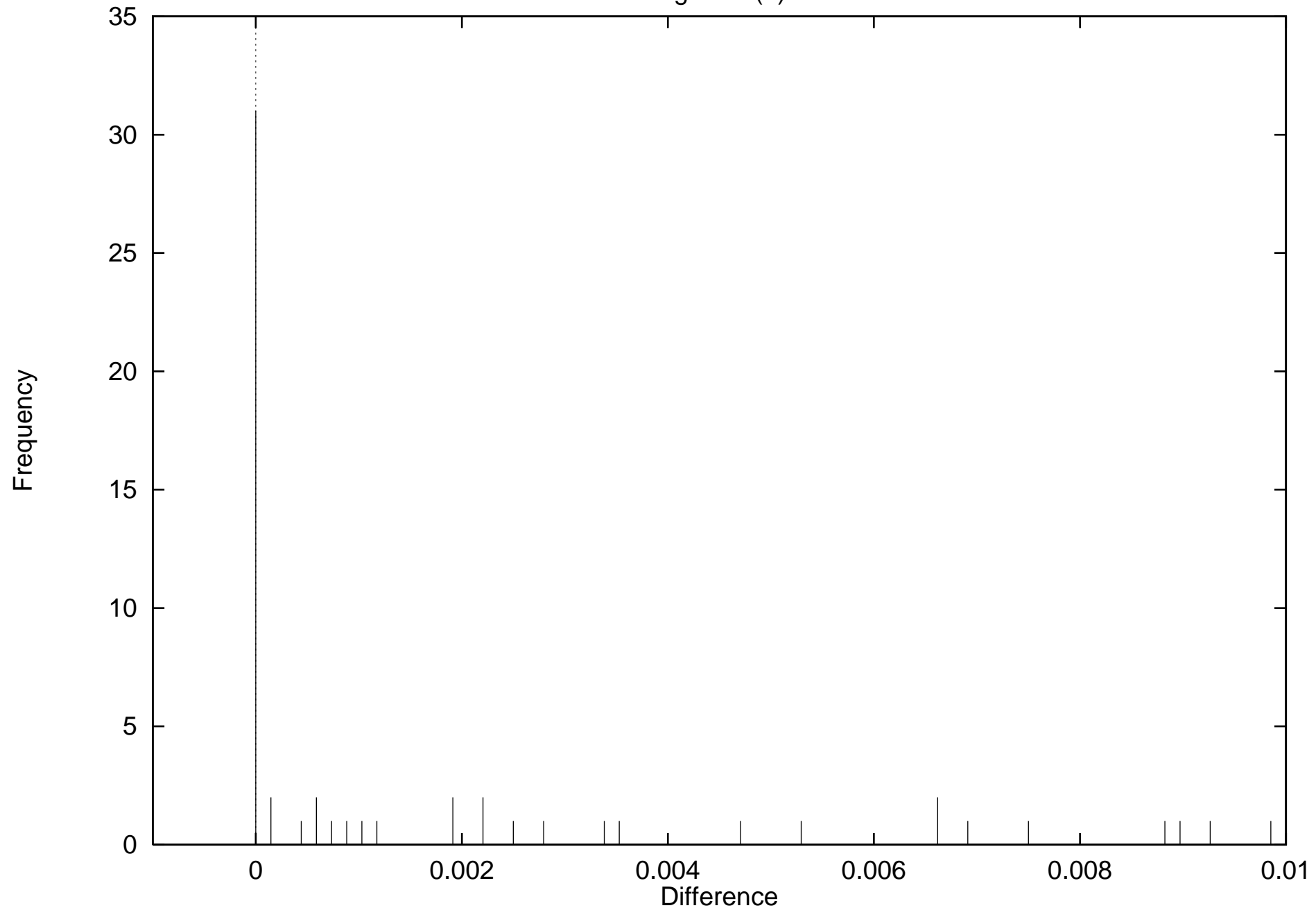


Figure 3 (a)

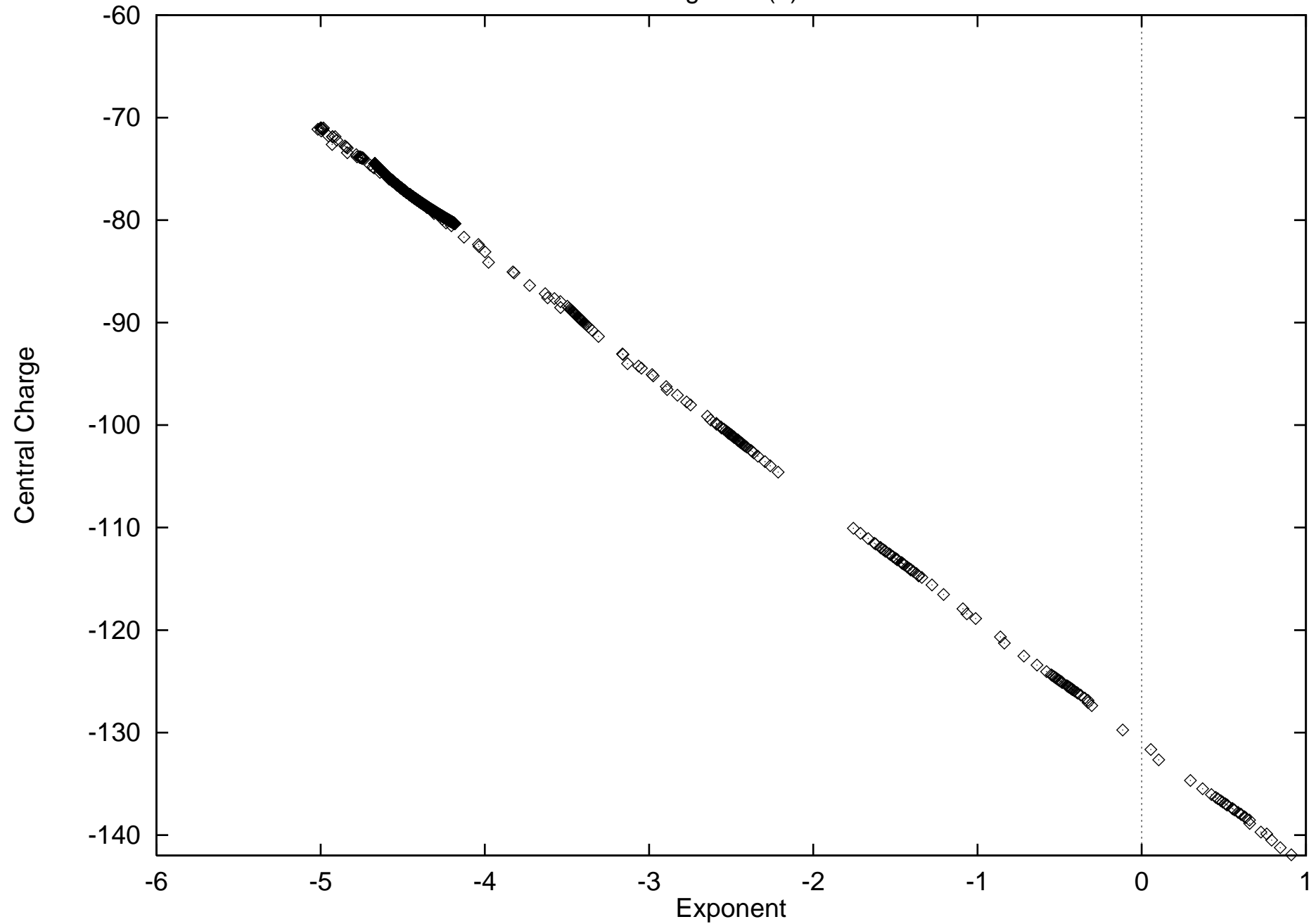


Figure 3 (b)

